

# Generic Contrast Agents

Our portfolio is growing to serve you better. Now you have a *choice*.



[VIEW CATALOG](#)

# AJNR

## **Appearance of Meningiomas on Diffusion-weighted Images: Correlating Diffusion Constants with Histopathologic Findings**

Christopher G. Filippi, Mark A. Edgar, Aziz M. Ulug, Joan C. Prowda, Linda A. Heier and Robert D. Zimmerman

This information is current as  
of May 7, 2025.

*AJNR Am J Neuroradiol* 2001, 22 (1) 65-72  
<http://www.ajnr.org/content/22/1/65>

# Appearance of Meningiomas on Diffusion-weighted Images: Correlating Diffusion Constants with Histopathologic Findings

Christopher G. Filippi, Mark A. Edgar, Aziz M. Uluğ, Joan C. Prowda, Linda A. Heier, and Robert D. Zimmerman

**BACKGROUND AND PURPOSE:** Malignant and atypical meningiomas are prone to recurrence and aggressive growth, which affects treatment planning and prognostication. Investigators have used diffusion-weighted imaging and apparent diffusion coefficient (ADC) maps to compare tumor grade and cellularity with the histopathologic findings of intraaxial primary brain neoplasms. The purpose of this study was to determine whether the signal characteristics of meningiomas on diffusion-weighted images correlate with the average diffusion constant ( $D_{av}$ ) from ADC maps and histopathologic findings and whether the  $D_{av}$  can reliably distinguish benign from malignant and atypical meningiomas.

**METHODS:** Seventeen patients (13 women and four men; average age, 55 years) with meningiomas were prospectively studied using routine MR imaging and diffusion-weighted imaging with a single-shot gradient-echo echo-planar pulse sequence (6000/100 [TR/TE]) and b values of 0 and 1000. Signal characteristics on routine MR and diffusion-weighted images were compared with the histopathologic findings after resection by using World Health Organization criteria.  $D_{av}$  values were calculated within the tumor mass from ADC maps before resection.

**RESULTS:** Four meningiomas were malignant or atypical (World Health Organization grades II and III).  $D_{av}$  values were lower than normal brain values (average,  $0.52 \pm 0.12 \times 10^{-5} \text{cm}^2/\text{s}$ ; range,  $0.45\text{--}0.69 \times 10^{-5} \text{cm}^2/\text{s}$ ) and were hyperintense on diffusion-weighted images and hypointense on ADC maps. Thirteen meningiomas were benign.  $D_{av}$  values were higher than normal brain values (average,  $1.03 \pm 0.29 \times 10^{-5} \text{cm}^2/\text{s}$ ; range,  $0.62\text{--}1.8 \times 10^{-5} \text{cm}^2/\text{s}$ ). On diffusion-weighted images and ADC maps, most were isointense. Five benign meningiomas had very high  $D_{av}$  values, bright signal on ADC maps, and distinct histopathologic findings, including microcysts, necrotic infarct, and organizing intratumoral hemorrhage. The difference in  $D_{av}$  values between malignant and benign meningiomas was statistically significant ( $P < .00029$ ).

**CONCLUSION:** Albeit a small sample size, meningiomas with low  $D_{av}$  tended to be malignant or highly atypical ( $P < .00029$ ) whereas meningiomas with the highest  $D_{av}$  had increased water content due to either a specific histologic subtype of meningioma or the presence of associated pathologic abnormality.

Meningiomas are readily diagnosed by MR imaging, and most are asymptomatic (1). Meningiomas comprise approximately 14% to 20% of all intracranial tumors (1, 2). Atypical meningiomas account for 7.2% of all meningiomas, whereas ma-

lignant meningiomas are rare and constitute approximately 2.4% (1). Malignant and atypical meningiomas are more prone to recurrence and aggressive growth, which increases patient morbidity and mortality (3–7). It would be useful to distinguish among benign, malignant, and atypical meningiomas before resection, because this would aid in surgical and treatment planning. This distinction between benign and malignant or atypical meningioma is neither easily nor reliably accomplished to date when assessing the imaging features of meningiomas on routine MR images (1, 2, 8–16).

Diffusion-weighted MR imaging has been used to investigate primary brain neoplasms. Correlations between apparent diffusion coefficient (ADC)

Received December 13, 1999; accepted after revision June 20, 2000.

J.C.P., L.A.H., R.D.Z.) and Pathology (M.A.E.), The New York Presbyterian Hospital-Weill Medical College of Cornell University, New York, NY.

Address reprint requests to Christopher G. Filippi, MD, Box 141, Department of Neuroradiology, 525 East 68th Street, New York, NY 10021.

© American Society of Neuroradiology

values, tumor cellularity, and tumor grade have been made (17–22), and the use of diffusion-weighted imaging to monitor treatment response has been evaluated (23). Whether diffusion-weighted imaging has a similar potential role in the diagnosis or prognosis of non-primary brain neoplasms or extraaxial neoplasms is unclear. The purpose of this study was to examine the signal characteristics of meningiomas prospectively on diffusion-weighted images and to correlate the  $D_{av}$  from the ADC maps preoperatively with the histopathologic findings after resection. We hypothesized that the calculated diffusion constant may be helpful in distinguishing benign from malignant and atypical meningiomas, and we hypothesized that the diffusion constant may be able to predict the histopathologic results of meningiomas.

## Methods

Between June 1998 and May 1999, 17 patients (13 women and four men; average age, 55 years) with meningiomas were prospectively studied using MR imaging and diffusion-weighted imaging. All of the patients had non-focal neurologic examinations at the time of presentation. Indications for MR imaging included headache (3), migraine (2), transient ischemic attack (5), change in mental status (4), and fall (1). Two patients underwent imaging as part of their routine follow-up for previous resection of meningiomas. These two patients were included because their initial MR examinations were performed before the availability of diffusion-weighted imaging. One of these patients had a benign meningioma, and the other had a meningioma that was initially interpreted as benign with atypical features.

All patients were studied using a 1.5-T whole-body MR imager equipped with high-performance gradients and manufacturer-supplied quadrature head coil. The standard imaging protocol consisted of the following sequences: sagittal T1-weighted (300/14), axial T1-weighted (500/12), fast spin-echo T2-weighted (3000/84), and axial fluid-attenuated inversion recovery (10002/162). After the administration of 0.1 mmol/kg gadopentetate dimeglumine, contrast-enhanced T1-weighted axial (450–500/12), and T1-weighted coronal (600/20) images were obtained. In all sequences, the field of view was 22 or 24 cm and the section thickness was 5 mm with an interslice gap of 2.5 mm.

Before the contrast-enhanced imaging was performed, routine diffusion-weighted MR images were obtained using single-shot multislice spin-echo echo-planar imaging for all patients. In the diffusion protocol, we used 10000/99 with b values of 0 and 1000 (24). For all images, a  $128 \times 128$  matrix size, 5-mm section thickness with no gap, and field of view of  $24 \times 24$  cm were used. In most studies, 30 images were obtained in an acquisition time of 42 s. The pulse sequence first obtained T2-weighted images without a diffusion-sensitizing gradient. Subsequently, diffusion-sensitizing gradients in the direction of the frequency-encoding, phase-encoding, and read-out gradients were used to generate three orthogonal diffusion-weighted echo-planar images.

The images were transferred to a workstation. An orientation-independent diffusion map ( $D_{av} = \text{Trace}/3 = [D_{xx} + D_{yy} + D_{zz}]/3$ ) was calculated for each pixel from the diffusion-weighted images. For each patient, average diffusion constants were then calculated from regions of interest within the tumor mass by using a voxel size of 5 mm.

Two neuroradiologists reviewed the MR and diffusion-weighted images without any knowledge of the histopathologic findings or the value of the calculated  $D_{av}$ . The signal intensity

of the meningiomas was assessed on the short- and long-TR images and the diffusion-weighted sequences. Signal intensity was judged as hypointense, isointense, slightly hyperintense, or hyperintense to cortex, and enhancement patterns were marked as either homogeneous or heterogeneous. Typical meningiomas had homogeneous signal intensity similar to that of gray matter, intense homogeneous enhancement (no cystic/necrotic/hemorrhagic foci), smooth and distinct margins, and no evidence of brain invasion. Any discrepancies in interpretation were resolved by consensus, and the reviewers were blinded before the consensus review.

A neuropathologist interpreted the histopathologic findings of the resected meningiomas and had no knowledge of the MR findings or values of the calculated  $D_{av}$ . Statistical analysis was conducted on the data sets by using a two-tailed Student's *t* test.

## Results

Seventeen patients with meningiomas were prospectively studied using standard MR pulse sequences and diffusion-weighted imaging with calculation of the diffusion constant ( $D_{av}$ ) within the tumor from ADC maps. The results are summarized in the Table.

In four (24%) of 17 cases, the meningiomas were malignant ( $n = 1$ ) or atypical ( $n = 3$ ). These meningiomas had markedly decreased diffusion constants, averaging  $0.53 \pm 0.12 \times 10^{-5} \text{ cm}^2/\text{s}$  and ranging in value from  $0.40$  to  $0.69 \times 10^{-5} \text{ cm}^2/\text{s}$ . In normal adult human brain tissue, the average  $D_{av}$  values are  $0.75 \pm 0.007 \times 10^{-5} \text{ cm}^2/\text{s}$  for white matter and  $0.76 \pm 0.11 \times 10^{-5} \text{ cm}^2/\text{s}$  for gray cortex (25, 26). All of these meningiomas were extremely hyperintense (“lightbulbs”) on the diffusion-weighted images and hypointense on the corresponding ADC maps.

Histopathologic examination revealed that one of these cases was classified as malignant or World Health Organization (WHO) grade III (Fig 1, patient 4). Brain invasion, multifocal areas of necrosis, hypercellularity, and cytologic pleomorphism with numerous abnormal mitoses were seen. This lesion had no atypical features on routine MR images; it had smooth, well-circumscribed borders and intense, homogeneous enhancement. Although this represented recurrent disease, the initial histopathologic examination revealed that this meningioma had typical features and was benign. Three of these meningiomas were classified as atypical (WHO grade II) based on histopathologic examination. These meningiomas contained multiple foci of tumor necrosis and the presence of a high mitotic rate as determined by the MIB-1 index. MIB-1 is a nuclear antigen expressed by all cycling cells, which is a measure of cell proliferation. Most tumors with an MIB-1 proliferation index greater than 10% show malignant histopathologic findings, and levels between 2% and 5% are usually atypical. The MR imaging characteristics of these tumors were typical of benign meningiomas, and atypical histopathologic findings were not anticipated on the basis of the MR imaging findings.

**Diffusion-weighted imaging and ADC map signal,  $D_{av}$  values, and histopathologic analysis of meningiomas**

Pt/Age/Sex	Location	Diffusion Images	ADC	D <sub>av</sub> Tumor 10 <sup>-5</sup> cm <sup>2</sup> /s	Histopathologic Findings
Group A					
1/66/F	Anterior falx	Hyperintense	Hypointense	0.4 (↓)	Malignant (WHO grade III)
2/48/M	Clivus	Hyperintense	Hypointense	0.69 (↓)	Atypical (WHO grade II)
3/26/F	Posterior falx	Hyperintense	Hypointense	0.54 (↓)	Atypical
4/45/F	Left parietal	Hyperintense	Hypointense	0.45 (↓)	Atypical
				Avg. 0.52 SD 0.1273	
Group B					
5/48/F	Anterior falx	Iso/hypointense	Iso/hyperintense	0.62 (↓)	Benign (WHO grade I)
6/55/F	Left parietal	Isointense	Isointense	0.80 (↑)	Benign
7/31/F	Anterior falx	Slightly hyperintense	Slightly hypointense	0.82 (↑)	Benign
8/48/F	Olfactory	Hypointense	Hyperintense	0.89 (↑)	Benign
9/49/F	Right temporal	Iso/hyperintense	Iso/hyperintense	0.93 (↑)	Benign
10/79/F	Anterior falx	Isointense	Isointense	0.94 (↑)	Benign
11/33/F	Right CP angle	Isointense	Isointense	0.96 (↑)	Benign
12/44/M	Left frontal	Isointense	Isointense	0.96 (↑)	Benign
13/77/F	Left frontal	Slightly hyperintense	Slightly hypointense	1.00 (↑)	Benign, microcystic
14/86/M	Left frontal	Hypointense	Hyperintense	1.07 (↑)	Benign, secretory
15/49/M	Left sphenoid	Hypointense	Hyperintense	1.26 (↑)	Benign, central infarct
16/85/F	Right sphenoid	Isointense	Isointense	1.32 (↑)	Benign, angiomatous
17/71/F	Left temporal	Hypointense	Hyperintense	1.80 (↑)	Benign, intratumor necrosis
				Avg. 1.03 SD 0.29	

Note.— $P < .00029$ , comparing average  $D_{av}$  of Group A (malignant/atypical meningiomas) vs Group B (benign meningiomas) by use of Student's two-tailed  $t$  test. Normal  $D_{av}$  for white matter:  $0.75 \pm 0.007 \times 10^{-5}$  cm<sup>2</sup>/s and normal  $D_{av}$  for gray cortex:  $0.76 \pm 0.11 \times 10^{-5}$  cm<sup>2</sup>/s (25, 26).

Thirteen (76%) of 17 meningiomas were benign as revealed by histopathologic examination (WHO grade I). On average, these meningiomas had an elevation in the diffusion constant (average,  $1.03 \pm 0.29 \times 10^{-5}$  cm<sup>2</sup>/s; range,  $0.62$ – $1.80 \times 10^{-5}$  cm<sup>2</sup>/s) (Fig 2, patient 9). These meningiomas were usually isointense on the short-TR images and predominantly hyperintense on the long-TR images. One of these benign meningiomas, which appeared densely calcified, had a diffusion constant below that of normal brain, overlapping the range of values observed in the malignant and atypical group. The other 12 meningiomas had diffusion constant values higher than that of normal brain, and none of these were densely calcified.

Five of these benign meningiomas had distinct histopathologic features. All of these meningiomas had the highest elevations in the diffusion constant (average  $1.29 \pm 0.22 \times 10^{-5}$  cm<sup>2</sup>/s), ranging in values from 1.07 to  $1.8 \times 10^{-5}$  cm<sup>2</sup>/s (Fig 3, patient 14). These meningiomas tend to be hypointense on diffusion-weighted images and hyperintense on ADC maps. Histopathologic analysis revealed that three of these meningiomas represented a benign subtype of meningioma with unique features. One of these meningiomas had undergone microcystic change, a feature of the histologic subtype called the microcystic meningioma. Another meningioma was classified as a secretory meningioma, which is another distinct subtype characterized by marked edema in the surrounding brain parenchyma. The third subtype was an angiomatous meningioma.

The other two meningiomas with elevated diffusion constants had distinctive histopathologic features. One contained a large central area of infarctlike necrosis. The other meningioma had organizing intratumoral hemorrhage with cystic degeneration. Albeit a small sample size, the difference in the diffusion constant of benign and malignant meningiomas was statistically significant ( $P < .00029$ ) using a Student's two-tailed  $t$  test.

### Discussion

Diffusion-weighted MR imaging has been evaluated as a diagnostic tool in cases of primary brain neoplasms. Tumor cellularity and tumor grade have been correlated with ADC values (the diffusion constant) from ADC maps (17–22). Primary brain neoplasms with higher cellularity or higher grades typically have lower ADC values or average diffusion constants when compared with normal brain tissue (17–22). Furthermore, the diffusion constant ( $D_{av}$ ) correlates with specific histopathologic features of high-grade gliomas. Cystic or necrotic portions of these tumors are associated with the highest  $D_{av}$  values (17). The ability of diffusion-weighted imaging to distinguish between peritumoral edema and unenhancing tumor reliably remains controversial (17, 22). Some groups have had success using ADC values to distinguish unenhancing tumor from peritumoral edema when the abnormality was located in white matter aligned parallel to the diffusion-weighted gradient. Other groups have been



FIG 1. Images of patient (patient 4 in the Table) with a malignant meningioma (WHO grade III).

A, Axial T1-weighted image (500/12/1) shows a well-marginated, recurrent extraaxial mass in the parietal convexity.

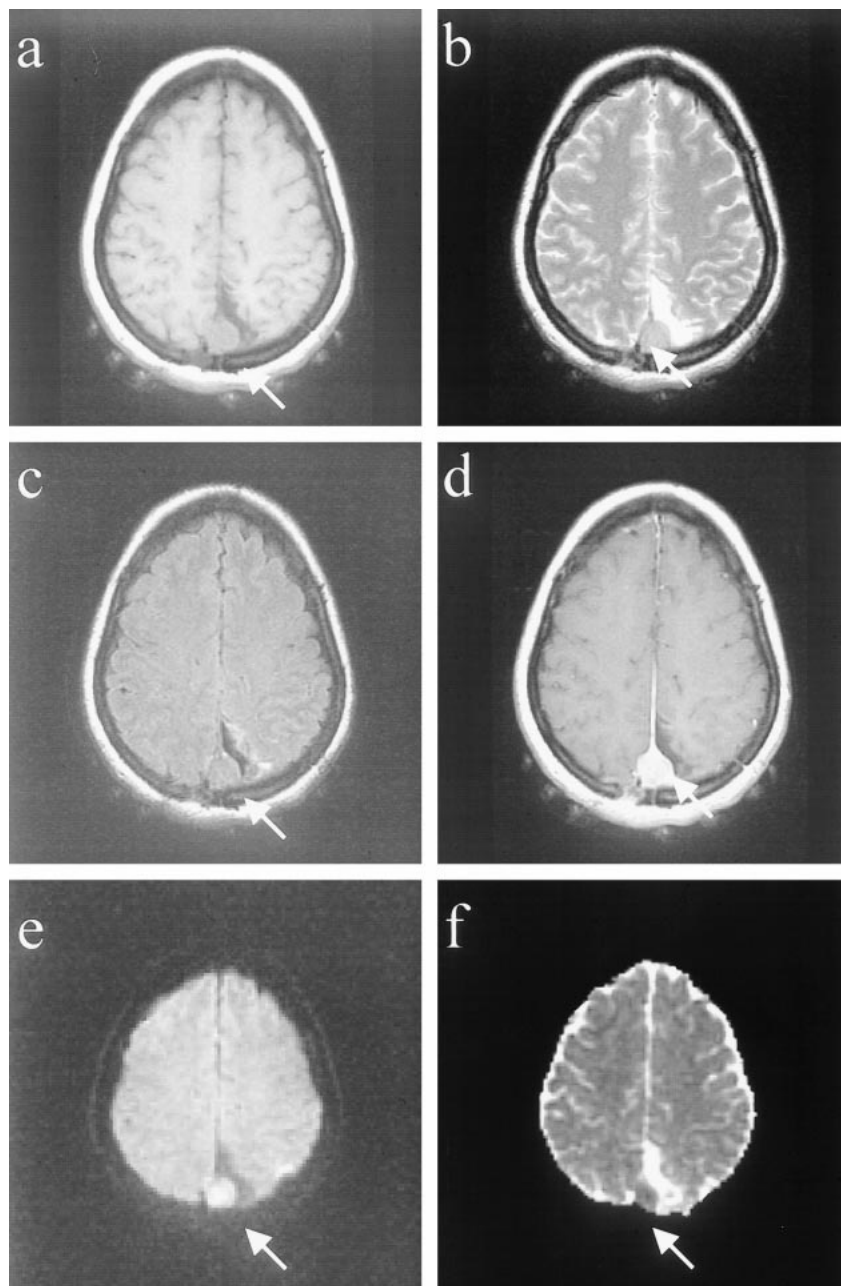
B, Axial fast spin-echo T2-weighted image (3000/84/1) of this recurrent meningioma appearing isointense to cortex.

C, Axial fast fluid-attenuated inversion recovery image (10002/162/1) shows isointense mass with smooth borders at resection site and no evidence of brain invasion.

D, Contrast-enhanced spin-echo T1-weighted image (450/12/1) shows smooth, homogeneous enhancement and dural enhancement typical of meningiomas.

E, Diffusion-weighted image (10000/99/1) of the recurrent meningioma, which is hyperintense (lightbulb).

F, Meningioma is hypointense on the ADC map, and the  $D_{av}$  was extremely low ( $0.45 \times 10^{-5} \text{ cm}^2/\text{s}$ ).



attempting to correlate  $D_{av}$  values from ADC maps on diffusion-weighted images with the response of primary neoplasms to treatment (23).

Because meningiomas are commonly occurring benign tumors that constitute approximately 20% of all intracranial tumors (1, 2) and are easily diagnosed using routine MR imaging, we chose to examine the signal characteristics of meningiomas on diffusion-weighted images prospectively and to correlate the  $D_{av}$  values from ADC maps preoperatively with histopathologic findings after resection. Furthermore, malignant and atypical meningiomas, although relatively uncommon and accounting for approximately 7.2% and 2.4% of all meningiomas, respectively (1, 2), are associated with less favorable clinical outcomes because they

are more prone to recurrence and aggressive growth (4–7). To date, investigators have been unsuccessful when attempting to predict the histologic or physical characteristics of meningiomas preoperatively, and there is no reliable way to distinguish benign from atypical or malignant meningiomas on routine MR images (1, 2, 8–16). Having the ability to distinguish benign from atypical or malignant meningiomas accurately would provide useful diagnostic information to aid in surgical and treatment planning and prognostication.

In this small series, most of the meningiomas ( $n = 13$ ) had benign results of their histopathologic examinations. According to the WHO classification of meningiomas, those meningiomas with low risk of recurrence and aggressive growth are classified

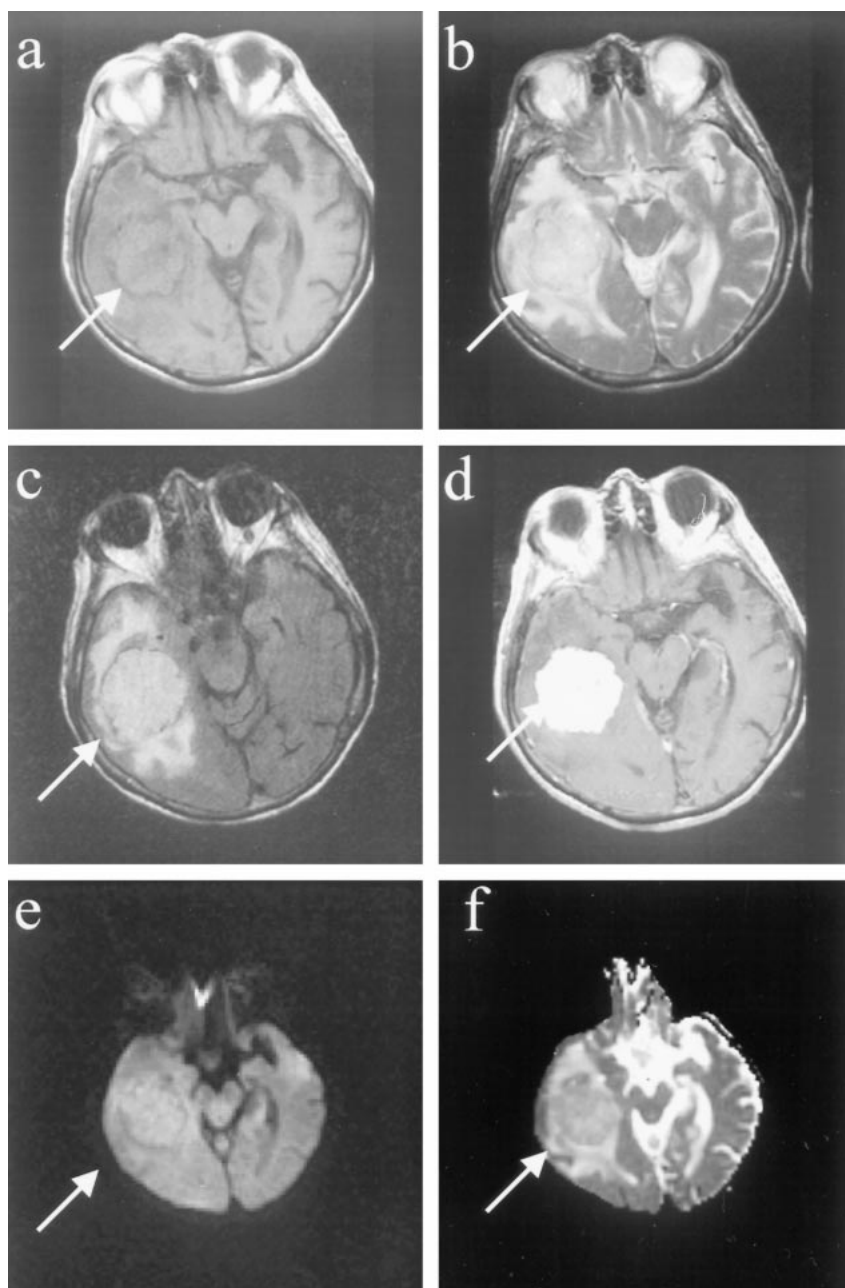


FIG 2. Images of a patient (patient 9 in the Table) with a benign meningioma (WHO grade I).

A, Axial T1-weighted image of right temporal meningioma with "pseudocapsule" sign.

B, Axial fast spin-echo T2-weighted image shows that the mass is slightly hyperintense to cortex.

C, Fast fluid-attenuated inversion recovery image shows mass to be hyperintense to cortex.

D, Contrast-enhanced T1-weighted image shows intense, homogeneous enhancement.

E, Mass is predominantly isointense/slightly hyperintense on the diffusion-weighted image.

F, On the ADC map, the mass appears isointense/hyperintense to cortex, with a diffusion constant value ( $0.93 \times 10^{-5} \text{ cm}^2/\text{s}$ ) that is slightly elevated compared with normal brain parenchyma.

as WHO grade I (4). The grade I classification includes the most common types of meningioma (fibrous or fibroblastic, transitional or mixed, and meningothelial) and the following benign subtypes: psammomatous, angiomatous, microcystic, secretory, lymphoplasmacyte-rich, and metaplastic (4).

The appearance of these 13 meningiomas on the diffusion-weighted images was variable. There were nearly equal numbers of meningiomas appearing hypointense, isointense, or hyperintense on the diffusion-weighted sequences and on the ADC maps. Furthermore, it is difficult to draw firm conclusions regarding any relationship between the appearances of these lesions on routine MR images and on diffusion-weighted images. In all cases, the meningiomas were isointense on the short-TR im-

ages, most appeared isointense to hyperintense on the long-TR images, and all enhanced homogeneously, as expected.

All except one of these benign meningiomas in our series had elevated diffusion constants compared with normal brain. Of note is that one meningioma showed a marked decrease in the diffusion constant. This meningioma exhibited benign but distinct histopathologic results. This particular meningioma was a psammomatous meningioma, which was completely densely calcified, as readily seen on MR images and CT scans. These meningiomas with abundant psammoma bodies form irregular calcified and occasionally ossified masses (4). The decreased diffusion constant may relate to the paramagnetic properties of calcium. It is rea-

FIG 3. Images of a patient (patient 14 in the Table) with a benign meningioma, distinct histopathologic subtype.

A, Axial T1-weighted image shows left frontal extraaxial mass with smooth margins and pseudocapsule sign.

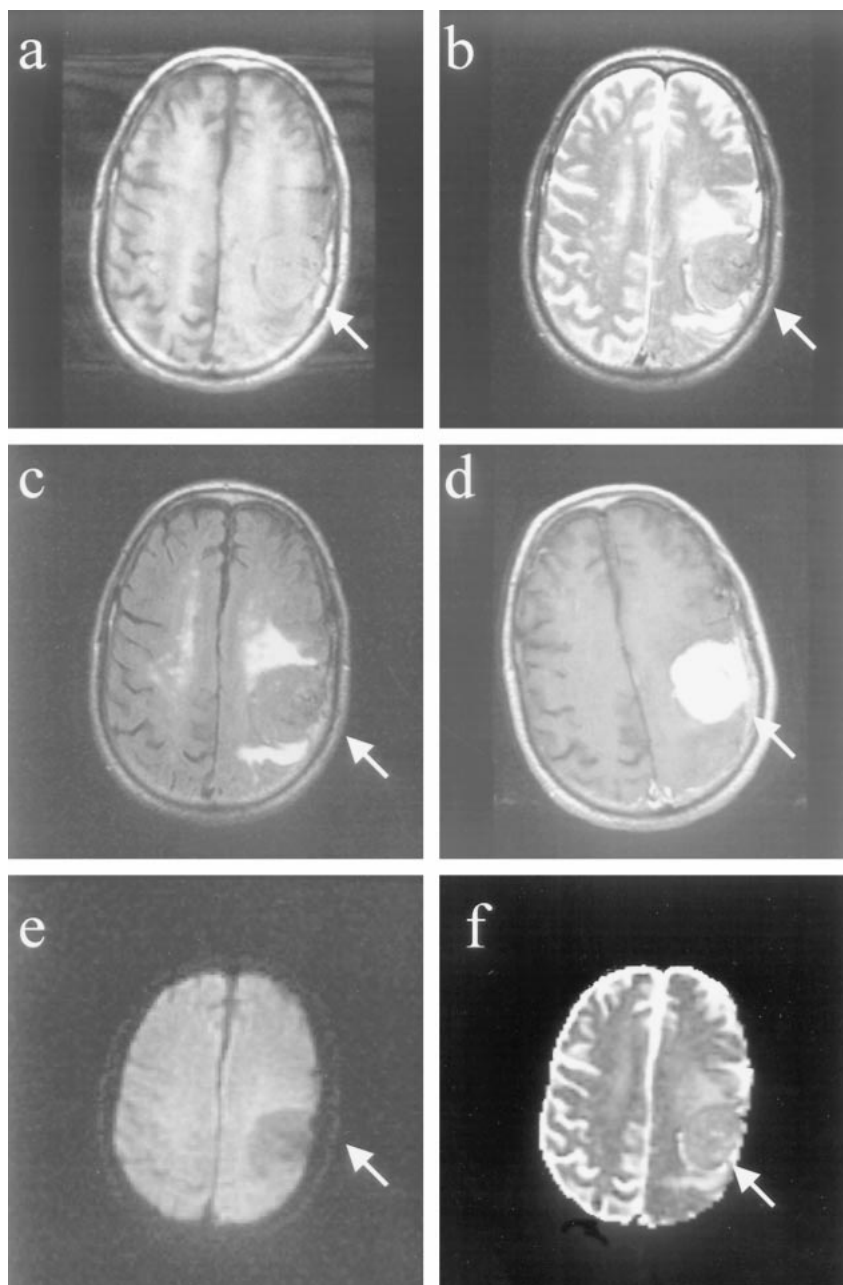
B, Fast spin-echo T2-weighted image of the mass is isointense to cortex, with areas of hypointensity.

C, Fast fluid-attenuated inversion recovery image shows that the mass is isointense to cortex.

D, Homogeneous enhancement and "dural tail" are seen on the contrast-enhanced axial T1-weighted image.

E, Diffusion-weighted image shows that the meningioma is hypointense.

F, On the ADC map, the lesion is predominantly hyperintense, with areas of isointensity. The diffusion constant of this meningioma was elevated ( $1.07 \times 10^{-5} \text{ cm}^2/\text{s}$ ). This is greater than a 25% elevation compared with normal brain parenchyma. Histopathologic analysis revealed that this represented a secretory meningioma, which produces brain parenchymal edema (seen best by the fast fluid-attenuated inversion recovery) and which has prominent pericytic proliferations.



sonable to postulate that a densely calcified mass would create a cellular environment in which the presence of this mineral would change the normal translational movement of water molecules across membranes.

In this study, it seems that the calculation of the diffusion constant from the isotropic diffusion map (ADC map) may reliably predict some histopathologic findings. For example, all five benign meningiomas with the highest elevations in the diffusion constant ( $D_{av} > 1.0 \times 10^{-5} \text{ cm}^2/\text{g}$ ) had distinct histopathologic features. One was a microcystic meningioma, which is rich in intracellular fluid and frankly cystic (27–30). Another meningioma was a secretory meningioma, which produces marked edema out of proportion to tumor size, which may

be related to the prominent pericytic proliferations often seen in this tumor type (27, 28, 31–33). There was an angiomatous meningioma, which is a distinct subtype that shows numerous blood vessels on the background of a typical meningioma (4). The other two meningiomas with this markedly elevated diffusion constant had unique features not normally seen in meningiomas, including one with a central infarction and one with organizing intratumoral hemorrhage and cystic degeneration. High-grade gliomas with cystic or necrotic portions had similar elevations in the diffusion constant (17). We hypothesize that all of these meningiomas showed hypointensity on the diffusion-weighted sequences and corresponding elevations in the diffusion constant because of the presence of increased amounts



of fluid within these lesions. The presence of the increased fluid may allow for freer movement of water molecules or less restriction to water diffusion, much in the same way that CSF diffuses freely without restriction and appears markedly hypointense on the diffusion-weighted MR sequences.

In this small series, there were four meningiomas that were malignant or atypical. Three were classified as atypical (WHO grade II), and one was classified as malignant (WHO grade III). According to WHO criteria, atypical meningiomas must have increased mitotic activity or three or more of the following: small cells with high nucleus to cytoplasmic ratio, prominent nucleoli, uninterrupted patternless or sheetlike growth, and foci of "spontaneous" or "geographic necrosis" (4). Increased mitotic activity has been defined as four or more mitoses per 10 high-power fields (4). To be classified as a malignant meningioma, the meningioma must exhibit features of frank malignancy. Such features include malignant cytology (eg, having an appearance similar to sarcoma, carcinoma, or melanoma) and a high mitotic index, which is defined as 20 or more mitoses per high-powered field (4).

All of the malignant or atypical meningiomas in this series had markedly increased signal on diffusion-weighted images, hypointense signal on the ADC maps, and extremely low diffusion constants indicative of marked restriction to water diffusion. All of these meningiomas had imaging characteristics suggestive of benign disease, which included homogeneous signal intensity similar to that of gray matter, intense homogeneous enhancement (no cystic/necrotic/hemorrhagic foci), smooth and distinct margins, and no evidence of brain invasion. Atypical or malignant histopathologic results were not anticipated on the basis of routine MR imaging.

It seems that the histopathologic findings of these atypical and malignant meningiomas correlated well with their appearance on diffusion-weighted images and the value of the calculated diffusion constant. These meningiomas showed hypercellularity, multifocal areas of necrosis, brain invasion, numerous abnormal mitoses, or cytologic pleomorphism. There are several possible explanations for this observed correlation. One factor is that malignant and atypical meningiomas have less extracellular water and space, which reduces the ADC value. This observation is expected if one considers that primary brain neoplasms, which have been treated, show an increase in extracellular water and space due to cell lysis (less viable and less cellular tumor), and this results in an increase in the diffusion constant (23). Furthermore, the histopathologic features that are unique to atypical and malignant meningiomas create a complex, local environment that imposes restrictions on the normal diffusion of water molecules within these lesions. These meningiomas have higher nuclear-to-cytoplasmic ratios and more prominent nucleoli, and this increased amount of intracellular, complex pro-

tein molecules likely restricts the free translation of intracellular water.

## Conclusion

Albeit a small sample size, atypical and malignant meningiomas tend to be markedly hyperintense on diffusion-weighted MR images and exhibit marked decreases in the diffusion constant ( $D_{av}$ ) or ADC values when compared with normal brain parenchyma. Although benign meningiomas have a variable appearance on diffusion-weighted images, they tend to have higher  $D_{av}$  values compared with normal brain, with the exception of densely calcified or psammomatous meningiomas, which may have a low  $D_{av}$ . Benign meningiomas with the highest  $D_{av}$  seem to have increased water content because of either a specific histologic subtype of meningioma or distinct histopathologic features. Furthermore, the average  $D_{av}$  values of malignant and atypical meningiomas were significantly lower compared with benign meningiomas ( $P < .00029$ ).

It seems that the quantification of the diffusion constant may reliably predict the histopathologic features of meningiomas before resection. Because atypical and malignant meningiomas are more prone to recurrence and aggressive growth, diffusion-weighted MR imaging with calculation of the diffusion constant should be performed when meningiomas are detected because this may provide useful diagnostic information for presurgical planning, treatment, and prognostication.

## References

1. Verheggen R, Finkenstaedt M, Bockermann V, Markakis E. **Atypical and malignant meningiomas: evaluation of different radiological criteria based on CT and MRI.** *Acta Neurochir (Wien)* 1996;65:66-69
2. Mahmood A, Caccamo DV, Tomecek FJ, Malik GM. **Atypical and malignant meningiomas: a clinicopathological review.** *Neurosurgery* 1993;33:955-963
3. Naumann M, Meixenberger J. **Factors influencing meningioma resection rate.** *Acta Neurochir (Wien)* 1990;107:108-111
4. Louis DN, Scheithauer BW, Budka H, von Deimling A, Kepes JJ. **Meningiomas.** In: Kleihues P, Cavenee WK, eds. *World Health Organization Classification of Tumours: Pathology and Genetics of Tumours of the Central Nervous System.* Lyon: IARC Press; 2000:176-184
5. Ayerbe J, Lobato RD, de la Cruz J, et al. **Risk factors predicting recurrence in patients operated on for intracranial meningioma: a multivariate analysis.** *Acta Neurochir (Wien)* 1999;141:921-932
6. Montriwathchai P, Kasantikul V, Taecholarn C. **Clinicopathological features predicting recurrence of intracranial meningiomas.** *J Med Assoc Thai* 1997;80:473-478
7. Kunicki A. **Relation of meningiomas to their nearest environment and its significance for recurrence of the tumor.** *Neuropatol Pol* 1986;24:511-520
8. Yamaguchi N, Kawase T, Sagoh M, Ohira T, Shiga H, Toya S. **Prediction of consistency of meningiomas with preoperative magnetic resonance imaging.** *Surg Neurol* 1997;48:579-583
9. Carpeggiani P, Crisi G, Trevisan C. **MRI of intracranial meningiomas: correlation with histology and physical consistency.** *Neuroradiology* 1993;35:532-536
10. Araki T, Inoue T, Suzuki H, Machida T, Iio M. **Magnetic resonance imaging of brain tumors: measurement of T1.** *Radiology* 1984;150:95-98



11. Elster AD, Challa VR, Gilbert TH, Richardson DN, Contento JC. **Meningiomas: MR and histopathologic features.** *Radiology* 1989;170:857-862
12. Zee CS, Chin T, Segall HD, Destian S, Ahmadi J. **Magnetic resonance imaging of meningiomas.** *Semin Ultrasound CT MR* 1992;13:154-169
13. Demaerel P, Wilms G, Lammers M, et al. **Intracranial meningiomas: correlation between MR imaging and histology in fifty patients.** *J Comput Assist Tomogr* 1991;15:45-51
14. Spagnoli MV, Goldberg HI, Grossman RI, et al. **Intracranial meningiomas: high-field MR imaging.** *Neuroradiology* 1986;161:369-375
15. Kallio M, Sankila R, Hakulinen T, Jaaskelainen J. **Factors affecting operative and excess long-term mortality in 935 patients with intracranial meningioma.** *Neurosurgery* 1992;31:2-12
16. Kepes JJ. **Meningiomas: biology, pathology, and differential diagnosis.** In: Kepes JJ, ed. *Masson Monographs in Diagnostic Pathology*. Masson: Masson Pub;1982:112-123
17. Eis M, Els T, Hoehn-Berlage M, Hossmann KA. **Quantitative diffusion MR imaging of cerebral tumor and edema.** *Acta Neurochir Suppl (Wien)* 1994;60:344-346
18. Gupta RK, Sinha U, Cloughesy TF, Alger JR. **Inverse correlation between choline magnetic resonance spectroscopy signal intensity and the apparent diffusion coefficient in human glioma.** *Magn Reson Med* 1999;41:2-7
19. Eis M, Els T, Hoehn-Berlage M. **High resolution quantitative relaxation and diffusion MRI of three different experimental brain tumors in rat.** *Magn Reson Med* 1995;34:835-844
20. Els T, Eis M, Hoehn-Berlage M, Hossmann KA. **Diffusion-weighted MR imaging of experimental brain tumors in rats.** *MAGMA* 1995;3:13-20
21. Sugahara T, Korogi Y, Kochi M, et al. **Usefulness of diffusion-weighted MRI with echo-planar technique in the evaluation of cellularity in gliomas.** *J Magn Reson Imaging* 1999;9:53-60
22. Tien RD, Felsberg GJ, Friedman H, Brown M, Mac Fall J. **MR imaging of high-grade cerebral gliomas: value of diffusion-weighted echoplanar pulse sequence.** *AJR Am J Roentgenol* 1994;162:671-677
23. Chenevert TL, Mc Keever PE, Ross BD. **Monitoring early response of experimental brain tumors to therapy using diffusion magnetic resonance imaging.** *Clin Cancer Res* 1997;3:1457-1466
24. Le Bihan D. **Diffusion NMR imaging with spin echoes.** In: Le Bihan D, ed. *Diffusion and Perfusion Magnetic Resonance Imaging: Applications to Functional MR*. New York: Raven Press; 1995:19-28
25. Uluğ A, van Zijl P. **Orientation-independent diffusion imaging without tensor diagonalization: anisotropy definitions based on physical attributes of the diffusion ellipsoid.** *J Magn Reson Imaging* 1999;9:804-813
26. Pierpaoli C, Basser P. **Toward a quantitative assessment of diffusion anisotropy.** *Magn Reson Med* 1996;36:893-906
27. Russell DS, Rubinstein L. **Pathology of Tumours of The Nervous System.** 4th ed. London: Edward Arnold;1977:65-100
28. Zulch KJ. **Brain Tumors, Their Biology and Pathology.** 3rd ed. New York: Springer;1986:357-382
29. Kleinman GM, Liszczak T, Tarlov E, Richardson EP, Jr. **Microcystic variant of meningioma: a light microscopic and ultrastructural study.** *Am J Surg Pathol* 1980;4:383
30. Michaud J, Gagne F. **Microcystic meningioma: clinicopathologic report of eight cases.** *Arch Path Lab Med* 1983;107:75
31. Challa VR, Moody DM, Marshall RB, Kelly DL, Jr. **The vascular component in meningiomas associated with severe cerebral edema.** *Neurosurgery* 1980;7:363
32. Philippon J, Foncin JF, Grob R, Srouf A, Poisson M, Pertuiset BF. **Cerebral edema associated with meningiomas: possible role of a secretory-excretory phenomenon.** *Neurosurgery* 1984;14:295
33. Mirra SS, Miles ML. **Unusual pericytic proliferation in a meningotheliomatous meningioma: an ultrastructural study.** *Am J Surg Pathol* 1982; 6:573-580